Astron. Astrophys. 359, 1117–1123 (2000)

ASTRONOMY AND ASTROPHYSICS

^{28}SiO, ^{29}SiO and ^{30}SiO excitation: effects of infrared line overlaps

F. Herpin* **and A. Baudry**

Observatoire de Bordeaux, B.P. 89, 33270 Floirac, France

Received 15 December 1999 / Accepted 17 May 2000

Abstract. We have investigated the influence of several line overlaps between ^{28}SiO, ^{29}SiO and ^{30}SiO on maser emission from the envelopes of late-type stars using the *Large Velocity Gradient* radiative transfer formalism modified to account for overlaps. Our model includes: (i) 40 rotational levels for each of the $v = 0$ to 4 vibrational states and each isotopic species; (ii) collisions with molecular and atomic hydrogen; and (iii) radiative pumping by a shell of dust grains surrounding the SiO masing layers.

We have shown that several line overlaps may play a role on the excitation of the ^{28}SiO $v = 3, J = 1 \rightarrow 0$ maser, and on the anomalously weak $v = 3, J = 2 \rightarrow 1$ emission. We suggest that ^{28}SiO maser emission in the $v = 4, J = 5 \rightarrow 4$ line, the only one observed in this vibrational level, may also result from line overlaps. For ^{29}SiO, infrared line overlaps successfully explain observed maser emission in the $v = 0, J = 5 \rightarrow 4$ and $v = 1, 2, J = 6 \rightarrow 5$ lines. ^{30}SiO, $v = 0, J = 2 \rightarrow 1$, and $v = 0, J = 4 \rightarrow 3$ maser emissions could also result from line overlaps, and we find that several overlaps could explain the newly discovered maser line ^{30}SiO $v = 1, J = 1 \rightarrow 0$. Finally, we make some predictions for new ^{28}SiO, ^{29}SiO and ^{30}SiO maser lines.

Key words: line: formation – masers – stars: circumstellar matter – stars: late-type

1. Introduction

SiO masers are excited in the inner layers of circumstellar envelopes of late-type stars, before the dust formation zone, but beyond the photosphere where outflow and inflow of matter or shocks coexist and give rise to complex physical conditions.

Since the discovery of SiO maser emission by Snyder & Buhl (1974), many papers have been published to explain the SiO maser phenomenon, and several improvements involving collisional and radiative pumping have been proposed to model the emission from late-type stars. However, it is still difficult to explain the disparities between some rotational line intensities observed inside a same vibrational state or, more generally, in adjacent transitions of ^{30}SiO, ^{29}SiO and $v \geq 3$ ^{28}SiO. Olofsson et al. (1981, 1985) introduced the hypothesis of a line overlap between two ro-vibrational lines of SiO and water to explain the weakness of the ^{28}SiO $v = 2, J = 2 \rightarrow 1$ emission. This emission was observed by Bujarrabal et al. (1996) in stars with different O-abundances, and the overlap between two infrared lines of H_2O and SiO was confirmed. In addition, several overlaps between the infrared lines of the main (^{28}SiO) and rare (^{29}SiO and ^{30}SiO) isotopic species of silicon monoxyde have been suggested to play a role in the excitation of these species. Using the *LVG* approximation Cernicharo et al. (1991) modeled the pumping of ^{29}SiO by ^{28}SiO. The importance of overlaps was further investigated by Cernicharo & Bujarrabal (1992) and Cernicharo et al. (1993). Recently, González-Alfonso et al. (1996) and González-Alfonso & Cernicharo (1997) used a non-local radiative transfer code to study the question of line overlaps. They successfully explained most of the ^{29}SiO, ^{30}SiO and high-v ($v \geq 3$) ^{28}SiO masers; however, several lines remain unexplained.

Our main goal in this work is to develop a simple and modular calculation tool in order to investigate the impact of various line overlap effects among the three main isotopic forms of SiO. We do not intend here to realistically model the SiO maser line profiles. We rather are interested in predicting and discussing relative peak line intensity ratios. In Sect. 2 we give details on spectroscopy, the used radiative transfer code and physical parameters, and on validation of our code. In Sect. 3, we include several line overlaps and compare our results to the observations. Some major results of this work are summarized in Sect. 4.

2. The model

The LVG code used here must be regarded as a simple but powerful computational tool for maser emission prediction. Bujarrabal (1994) has clearly demonstrated that the LVG code applied to the SiO maser zone is a fairly good approximation in comparison with the exact radiative transfer solution. Other uncertainties do not play a minor role in comparison with the differences between the LVG and the exact radiative transfer results; in particular uncertainties in the collision laws and the exact geometry of the maser region result in weaker predictions. Thus, we be-

Send offprint requests to: F. Herpin (herpin@isis.iem.csic.es)

* *Present address:* Dept Física Molecular, I.E.M., C.S.I.C, Serrano 121, 28006 Madrid, Spain

lieve that the physical laws and the spherical symmetry adopted in our model are sufficient for the LVG approximation.

2.1. Spectroscopy, collisions and radiative transfer

Modeling the SiO emission requires the use of accurate spectroscopic data and collisional rates. Energy levels of SiO have been calculated using the most recent calculations of the Dunham coefficients (Campbell et al. 1995). For the Einstein A-coefficients we used the recent work of Drira et al. (1997).

Basic data concerning the rotational and rovibrational rate coefficients of SiO with H_2 and their dependence on temperature were taken from Bieniek & Green (1983). We also used the new rate coefficients derived by Lockett & Elitzur (1992) for $v \geq 3$ and $\Delta v = 2$ transitions and we applied corrections to their rates to compensate for the effect of the limited number of rotational and vibrational levels taken in the calculations. In addition, Langer & Watson (1984) made a first attempt to estimate collision rates of SiO with atomic hydrogen from a comparison with the expected H-CO and H_2-CO rates. The main features of these H-SiO rates used in our work are: the vibrational collision rates are 10 times larger than those for H_2, and the rotational collision rates are decreased by a factor of 7. H can be formed in two different ways: (*i*) the stellar radiation may photodissociate H_2 close to the star, thus forming an atomic hydrogen layer; (*ii*) shocks may dissociate H_2 to produce a uniform distribution of H throughout the envelope. We assume here that $\chi[H_I/H_2]$ is constant and equal to 10^{-2} as in Bowers & Knapp (1987). Adding atomic hydrogen to H_2 increases the role of collisions. Note however that its impact on the inversions is weak (a few % for $\chi[H/H_2] < 10^{-1}$). Beyond this value, inversions for the lowest rotational levels tend to decrease contrary to what is observed for high J transitions. The higher the vibrational level, the larger the effect of the atomic hydrogen is; this is expected because of larger vibrational collision rates for H than for H_2. Nevertheless, we stress that these collision rates and the relative abundance of the atomic hydrogen are poorly known.

Because the purpose of this work is to explain in a simple way the main characteristics of ^{28}SiO, ^{29}SiO and ^{30}SiO emissions, we have used the *LVG* (Sobolev 1958) approximation, based on the model of a homologously expanding envelope, in which the escape probability does not depend on the angle. If the velocity gradient (logarithmic velocity gradient $\varepsilon_r = d\ln V/d\ln r$) in the circumstellar envelope is large enough, each cell of the discretized medium will be decoupled from all other cells, thus allowing a local treatment of the radiative transfer. The interaction area is limited to a small zone where photons can be absorbed or emitted around a resonance point. We have limited the maximum size of the cells to the *Sobolev length*, L, defined by

$$L = r\frac{\Delta V_D/V}{\varepsilon_r}$$

with

$$\Delta V_D = \sqrt{{\Delta V_{th}}^2 + {\Delta V_{turb}}^2}$$

where r is the radial distance, ΔV_{th} the thermal velocity, ΔV_{turb} the turbulence, and V the expansion velocity. ΔV_D characterizes the local absorption coefficient. The formula giving the Sobolev length applies to any form of expansion velocity and to the general case in which the photon escape probability depends on the direction. For a spherically symmetric envelope and for the special case where V is proportional to r, the angle-dependent terms vanish, the logarithmic gradient $\varepsilon_r = 1$, and the escape probability is isotropic and proportional to the inverse of the peak opacity (as soon as the opacity becomes large). The Sobolev length is just the length over which the velocity varies by an amount corresponding to the width of the local absorption coefficient. One essential advantage of the LVG code is that it requires less computer time than more exact treatments of the radiative transfer problem based on integral solutions (Bujarrabal 1994) or on the Monte Carlo method (González-Alfonso & Cernicharo 1997). In the frame of the LVG formalism and for physical conditions relevant to the circumstellar environment of late-type stars we have derived the solutions of the statistical equilibrium equations and the opacities of various SiO lines. More complex effects related to non spherical geometry, polarization or saturation and beaming angles are beyond the scope of this paper. Concerning saturation, we emphasize that our rate equations are solved for both positive and negative opacities, but that beaming related to saturation cannot be investigated here because we assume the escape probability to be isotropic. Note that beaming angles for saturated masers in the case of the *LVG* approximation remain an unsolved problem (Elitzur 1992). Saturation and the effect of competitive gains in SiO lines were investigated in Doel et al. (1995).

Our calculations include 40 rotational levels for each of the 5 vibrational states $v = 0$ to 4. To correct for the limited number of rotational and vibrational levels (this overestimates the opacities), we have applied a correction similar to that used by Bujarrabal & Nguyen-Q-Rieu (1981) for the rotational populations. The required final precision on the populations is better than 10^{-4}. Calculations are done simultaneously for ^{28}SiO, ^{29}SiO and ^{30}SiO. We derive the populations for each level (v, J) and derive the opacities for all allowed transitions.

2.2. Circumstellar parameters

We have used physical parameters appropriate to the circumstellar environment of evolved stars (see details in Herpin 1998).

$*$ *Kinetic temperature.* The gas temperature follows the law adopted by Langer & Watson (1984):

$$T_c = T_\star(\frac{r}{R_\star})^{-0.5}$$

where $R_\star$ is the stellar radius ($R_\star = 7.7\,10^{13}$ cm), $T_\star$ is the stellar temperature ($T_\star = 2500$ K) and r is the radial distance. This law is in rough agreement with the observations of SiO thermal emission of Lucas et al. (1992) and Bujarrabal et al. (1986), and also with the calculations of Willson (1987) who finds 1500 K

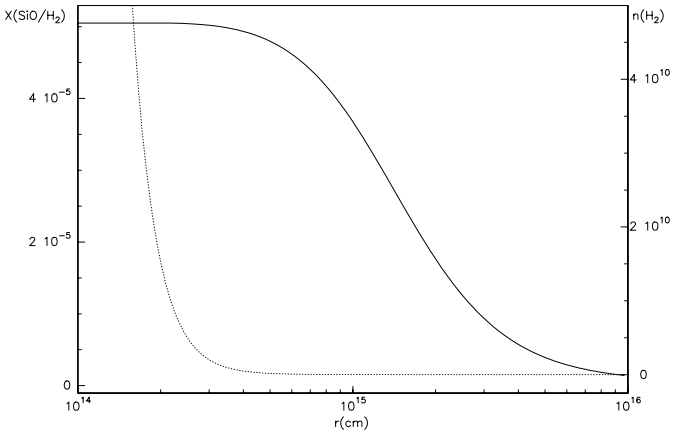

Fig. 1. SiO/H_2 abundance χ (continuous line) and H_2 density (in cm^{-3}, dotted line) versus the distance to the star r(cm) for $\chi_0 = 5\ 10^{-5}$, $\frac{dM}{dt} = 5.3\ 10^{-7}$ $M_\odot$/yr and $R_\star = 7.7\ 10^{13}$ cm.

in the maser region, for a typical Mira. Turbulence is a free parameter in our code and contributes to net line broadening.

∗ *Expansion velocity.* The expansion velocity of the gas adopted in our model is:

$$V = V_\infty \frac{1}{1 + (\frac{R_{acc}}{r})^{e_v}}$$

where $R_{acc} = 1.8\ 10^{15}$ cm, $e_v \in [1;3]$ and V_∞ is the asymptotic expansion velocity of the gas (9.5 km s^{-1}). A logarrithmic velocity gradient of 3 was used in the calculations.

∗ *SiO abundance.* The SiO/H_2 abundance ratio is uncertain, and we adopt the solar abundance by default ($\chi_0[SiO/H_2] = 5.\ 10^{-5}$). This abundance decreases with the distance to the star, the SiO molecules being progressively condensed onto the grains. We follow the law adopted by Bujarrabal et al. (1989), and we adopt for the ^{29}SiO and ^{30}SiO isotopic abundances (A_i) relative to ^{28}SiO, $1/19.5$ and $1/29.5$, respectively (see Fig. 1):

$$\chi(r) = \chi_0[1 - \frac{\kappa(r)}{\kappa_0} + \chi']/A_i$$

with χ_0 the initial ratio (here the solar abundance), and χ' the remaining fraction of SiO after the grain formation (10^{-2}). The terms $\kappa(r)$ and κ_0 depend respectively on the radiative pressure and the total quantity of grains formed. We take:

$$\kappa(r) = \kappa_0 \frac{(r - R_1)^2}{(r - R_1)^2 + (R_d - R_1)^2}$$

where R_d is the radius where half the total quantity of grains is formed ($1.5\ 10^{15}$ cm), and R_1 is the initial point ($2.\ 10^{14}$ cm).

∗ *H_2 density.* We adopt (Elitzur 1992):

$$n_{H_2} = \frac{\dot{M}}{8\pi r^2 V m_p}$$

with V the expansion velocity, $\dot{M}$ the steallar mass loss rate and m_p the proton mass (see Fig. 1). Maser effects will require densities of a few 10^9 particles/cm^3, whereas thermalization is clearly reached beyond $10^{10} - 10^{11}$ particles/cm^3.

∗ *Grain radiation.* IR spectra from the envelopes of late-type stars show that circumstellar grains have various chemical compositions. Here we only consider silicate grains and we assume that most circumstellar grains lie in a shell outside the SiO maser zone (with $R_{in} = 10^{15}$ cm, and $R_{out} = 10^{16}$ cm). The extinction coefficient of the dust is $Q_\nu \simeq Q_0(\frac{\lambda}{\lambda_0})^{-p}$ with $p \in [1;2]$ for wavelengths $\lambda \geq 1\,\mu$m (Mathis 1990). For silicate grains, we take $p = 1.1$, $\lambda_0 = 80\,\mu$m, and $Q_0 = 2.10^{-3}$ according to the work of Ivezic & Elitzur (1995). We consider that the silicate grains behave as black-bodies with temperature T_d. We assume that the dust is optically thin, and that T_d is constant throughout the envelope (T_d =600 K). We take, following Netzer & Elitzur (1993), $\chi_d = \frac{M_{dust}}{M_{H_2}} = 10^{-2}$, 3.0 g.$cm^{-3}$ for the grain volumic density, and 5.10^{-6} cm for the grain radius.

2.3. Line overlaps

In this work, we only deal with local line overlaps due to thermal line broadening and local turbulence in successive circumstellar layers. For simplicity, two nearby spectral lines are considered to overlap when $\Delta V \leq \Delta V_0$ where ΔV is the difference in velocity between the line centers, and ΔV_0 is an *a priori* fixed value. In the examples discussed in Sect. 3 we have adopted $\Delta V_0 = 5$ km s^{-1} corresponding to turbulent inner layers ($\Delta V_{thermal} \simeq 1.2$ km s^{-1}). Line overlaps are treated in a very simple manner. For two nearby lines ν_{12} and ν_{34}, we derive the opacities τ_{12}, τ_{34}, and the individual source functions S_{12}, S_{34}. Adding the absorption and emissivity coefficients of each line, the source function becomes

$$S_{12}{}' = S_{12}(\frac{\tau_{12}}{\tau_{12} + \tau_{34}}) + S_{34}(\frac{\tau_{34}}{\tau_{12} + \tau_{34}})$$

and the total opacity is now $\tau_{12}{}' = \tau_{12} + \tau_{34}$. The average intensity is then given by:

$$\overline{J}_{12} = [1 - \beta_{12}{}'(\tau')]S_{12}{}' + \beta_{12bb}{}'(\tau')I_{bb}$$

$$+\beta_{12bg}{}'(\tau')(I_{bg} + I_{dust})$$

where β is the usual escape probability. The cosmic background I_{bg} is described by a 3 K blackbody and the dust contribution is given by I_{dust}. The emission of the central star I_{bb} is described by a blackbody spectrum at temperature $T_\star$; a geometrical dilution factor is applied. In these formulae, the populations of the *4 levels* are involved. If $\tau_{12} < \tau_{34}$, after overlap we have $S_{12}{}' = S_{34}{}' \simeq S_{34}$ and $\tau'_{34} \simeq \tau_{34}$; this implies minor changes for τ_{34} and the n_3 and n_4 populations. On the other hand, photons from the stronger line will be absorbed by the more optically thin line 1–2, thus enhancing the non-equilibrium distribution of the populations in the levels 1 and 2.

Such a treatment of the overlaps is oversimplified, but allows us to test quickly the effects of this mechanism. Our code

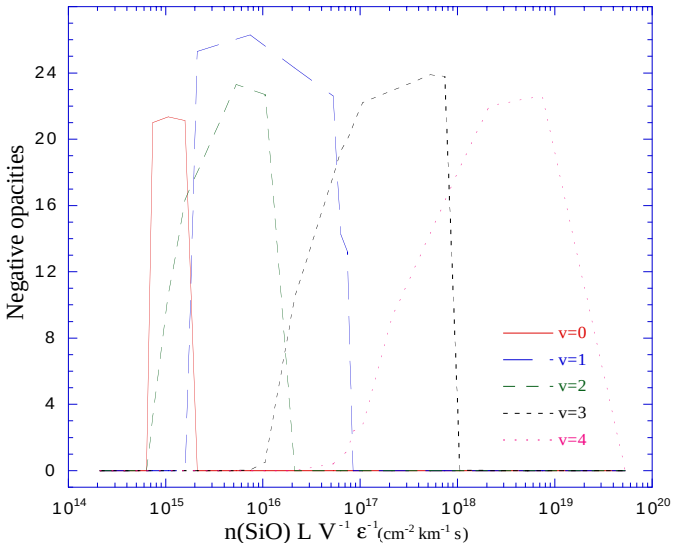

Fig. 2. ^{28}SiO negative opacities for the transition $J = 1 \rightarrow 0$ in $v = 0$ to 4. We have taken $T_\star = 2500$ K, $R_\star = 7.7\ 10^{13}$ cm, the logarithmic velocity gradient $\varepsilon = 3$ and $\frac{dM}{dt} = 5.3\ 10^{-8}$ M$_\odot$/yr. (The H_2 density is fixed to 10^9 cm^{-3} at a distance of $2.8R_\star$.) V is the expansion velocity.

incorporates three overlaps simultaneously; this number can of course be increased. To account for line overlaps, the code first derives the populations and opacities separately for each isotope without overlap, and then solves again for the radiative transfer, combining the overlapping lines. We describe in Sect. 3 how we proceed to test the effects of line overlaps.

In fact, non local line overlaps have long been recognized as important in the excitation of the OH radical, and, more recently, in SiO models (cf. Introduction and Sect. 3). Line overlaps may occur even if two lines are not excited in immediately adjacent gas layers; e.g. a Doppler-shifted line emitted from a first cloud may interact with another line in a second cloud provided that the two clouds have the appropriate relative velocities. In a somewhat different process, Olofsson et al. (1981, 1985) suggested that the anomalously weak $v = 2, J = 2 \rightarrow 1$ emission line in stars could be explained by non local overlap with the $H_2O\ \nu_2\ 12_{75} \rightarrow \nu_1\ 11_{66}$ line. Photons emitted by the water line increase the radiation field at the frequency of the vibrational transition of SiO creating an excess of absorption for this SiO line, and thus destroying the inversion in $v = 2, J = 2 \rightarrow 1$. This mechanism was recently investigated in detail by Bujarrabal et al. (1996).

2.4. Model validation

To test the validity of our code, we have used the same initial conditions as in Alcolea et al. (1989). (For this comparison, we have not applied corrections on the collision rates for the limited number of levels.) The main differences with Alcolea et al. are the number of rotational levels (40 here compared to 12 in Alcolea et al.), the collision rates (Langer & Watson 1984 in Alcolea et al.), and the more recent spectroscopic coefficients used here. In Fig. 2, we plot the $J = 1 \rightarrow 0$ negative opacities for $v = 0$ to 4 versus the ratio $n(SiO)LV^{-1}\varepsilon^{-1}$ (where L is the Sobolev length, V the expansion velocity, ε the logarithmic velocity gradient). Our results are much similar to those of Alcolea et al. and show that the $J = 1 \rightarrow 0$ inversions are well differenciated according to the vibrational state. However, some minor discrepancies remain. In particular, our work shows that $v = 1$ inversions occur over a broader range of parameters. We do not obtain increasing opacities with increasing v; but in Alcolea et al. this trend was probably the consequence of their smaller number of rotational levels. Finally, we note that results in Fig. 2 are similar to those of Lockett & Elitzur (1992).

3. Discussion of line overlap effects

Standard radiative and collisional SiO pumping models are able to predict several of the observed features of SiO maser emission from late-type stars (e.g., Bujarrabal 1994). These models predict similar line profiles and smooth line strength variations when one goes up the rotational energy ladder. They cannot explain, however, the anomalous line intensity ratios observed among several adjacent rotational transitions in high v states of ^{28}SiO and in $v = 0$ to 3 states of ^{29}SiO and ^{30}SiO. On the other hand, line overlap effects may strongly modify the SiO populations and thus explain apparent line anomalies. The most complete work in this domain (González-Alfonso et al. 1996, González-Alfonso & Cernicharo 1997) includes a non-local treatment of line overlap effects. Their model correctly predicts several observed features. It also predicts excitation of the ^{29}SiO $v = 3, J = 8 \rightarrow 7$ transition which was subsequently detected (González-Alfonso & Cernicharo 1997) thus demonstrating the importance of line overlaps. Nevertheless, excitation of several transitions remains unexplained in the work of González-Alfonso et al. In particular, emission from ^{29}SiO $v = 0, J = 5 \rightarrow 4$ and $v = 1, 2, J = 6 \rightarrow 5$ and ^{30}SiO $v = 0, J = 2 \rightarrow 1$ and $4 \rightarrow 3$ must be understood (see discussion below and Table 1).

The present model is conceived as a simple tool to quickly investigate the impact of various line overlaps between rovibrational lines of ^{28}SiO, ^{29}SiO and ^{30}SiO. The model incorporates up to 3 simultaneous different overlaps, namely six lines, according to the simple prescription outlined in Sect. 2.3. Once the maximum line shift allowed between two lines is fixed (this depends on ΔV_0 defined in Sect. 2.3), a specific module of our code searches for all possible overlaps. Within the 10 first rotational transitions we find a total of 27, 48 and 79 overlaps for $\Delta V_0 = 5, 10$ and 15 km s^{-1}, respectively. There are of course more overlaps involving higher J rotational levels, and we have also explored the influence of high J-level transitions overlapping low J-level transitions. As briefly explained in Sect. 2.3, the effect of a line overlap between two lines strongly depends on the relative strength of these two lines. In general, when an overlap occurs between ^{28}SiO and ^{29}SiO or ^{30}SiO transitions, the rare isotopic transitions which are optically thin tend to be more affected than the ^{28}SiO transitions; and the impact on the more optically thin lines is higher for lower v states. Our code derives the net optical depths compared to the non-overlapping

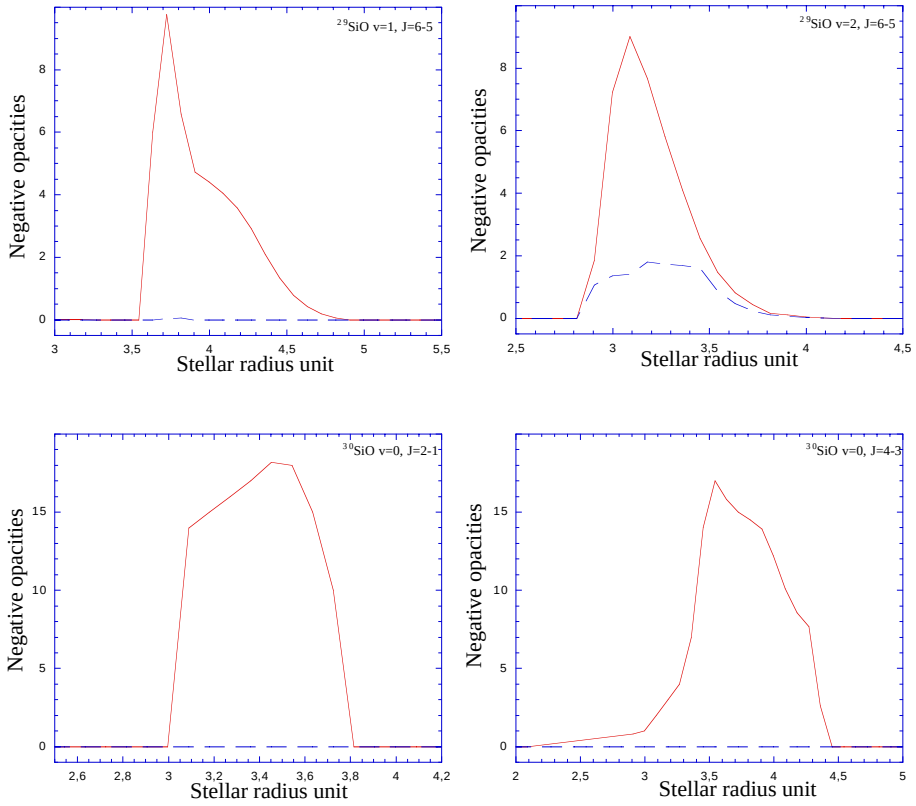

Fig. 3. Negative opacities of newly explained maser lines for ^{29}SiO (top) and ^{30}SiO (bottom) with (continuous line) and without (dashed line) overlap, versus the distance to the star (one stellar radius = 7.7 10^{13} cm). The overlaps used in these computations are given in bold face in Table 1. The H_2 density and the abundance $\chi[SiO/H_2]$ are respectively 10^9 cm^{-3} and 5 10^{-5} at a distance of $2.8R_\star$.

Table 1. Possible explanations of observed maser lines not explained in previous works. The overlaps used in Figs. 3 and 4 are given in bold face. Note the ^{30}SiO $v = 1, J = 1 \rightarrow 0$ maser line newly discovered by Cho & Ukita (1998).

Explained maser lines	**Overlaps**
^{29}SiO $v = 0, J = 5 \rightarrow 4$ (weak)	• ^{29}SiO $v = 1 - 0, J = 1 - 0$ + ^{28}SiO $v = 2 - 1, J = 4 - 3$
^{29}SiO $v = 1, J = 6 \rightarrow 5$	• ^{28}SiO $v = 2 - 1, J = 4 - 3$ + ^{29}SiO $v = 1 - 0, J = 1 - 0$ and ^{28}SiO $v = 2 - 1, J = 5 - 4$ + ^{29}SiO $v = 1 - 0, J = 2 - 1$ • ^{28}SiO $v = 3 - 2, J = 2 - 3$ + ^{29}SiO $v = 2 - 1, J = 5 - 6$ • ^{29}**SiO v = 2 − 1, J = 15 − 14** + ^{29}**SiO v = 1 − 0, J = 6 − 5**
^{29}SiO $v = 2, J = 6 \rightarrow 5$	• ^{30}**SiO v = 1 − 0, J = 1 − 0** + ^{29}**SiO v = 1 − 0, J = 3 − 4** • ^{28}SiO $v = 3 - 2, J = 2 - 3$ + ^{29}SiO $v = 2 - 1, J = 5 - 6$
^{30}SiO $v = 0, J = 2 \rightarrow 1$	• ^{30}**SiO v = 1 − 0, J = 1 − 0** + ^{29}**SiO v = 1 − 0, J = 3 − 4** • ^{28}SiO $v = 2 - 1, J = 3 - 4$ + ^{30}SiO $v = 1 - 0, J = 1 - 2$
^{30}SiO $v = 0, J = 4 \rightarrow 3$	• ^{28}**SiO v = 2 − 1, J = 3 − 4** + ^{30}**SiO v = 1 − 0, J = 1 − 2**
^{30}SiO $v = 1, J = 1 \rightarrow 0$	• ^{30}SiO $v = 1 - 0, J = 1 - 0$ + ^{29}SiO $v = 3 - 2, J = 11 - 10$ and ^{29}SiO $v = 3 - 2, J = 11 - 10$ + ^{28}SiO $v = 2 - 1, J = 2 - 3$ • ^{29}**SiO v = 1 − 0, J = 3 − 4** + ^{30}**SiO v = 1 − 0, J = 1 − 0** • ^{28}SiO $v = 2 - 1, J = 3 - 4$ + ^{30}SiO $v = 1 - 0, J = 1 - 2$

cases. Taking $\Delta V_0 = 5$ km s^{-1} results in 31 overlapping line pairs. These overlaps affect ^{28}SiO, ^{29}SiO or ^{30}SiO rotational transitions with $v \leq 4$ and $J \leq 10$. There is however the interesting case of ^{28}SiO $v = 2 - 1, J = 3 \rightarrow 4$ which requires $\Delta V_0 \simeq 10$ km s^{-1} to overlap with ^{30}SiO $v = 1-0, J = 1 \rightarrow 2$.

Because of radiative pumping through high v levels, we stress that very different (v, J) levels are connected. That is why some infrared overlaps have sometimes a strong influence on ro-vibrational levels not involved in these overlaps: because of this excitation mechanism numerous very different levels are connected together.

We have grouped our results into four categories: (*i*) the overlaps invoked by González-Alfonso et al. (1996) and González-Alfonso & Cernicharo (1997) to explain some important newly discovered rotational transitions; (*ii*) the overlaps which may account for the behaviour of maser rotational transitions explained elsewhere by other models and other overlaps; (*iii*) the overlaps

Table 2. Predicted new maser transitions. The lines in bold face have not been searched for maser emission as far as we are aware.

^{28}**SiO**	$v = 4$	$\mathbf{J = 3 \rightarrow 2}$
		$J = 4 \rightarrow 3$
^{29}**SiO**	$v = 0$	$J = 4 \rightarrow 3$
	$v = 1$	$J = 2 \rightarrow 1$
		$J = 5 \rightarrow 4$
	$v = 2$	$\mathbf{J = 1 \rightarrow 0}$
		$\mathbf{J = 3 \rightarrow 2}$
	$v = 3$	$\mathbf{J = 2 \rightarrow 1}$
		$\mathbf{J = 4 \rightarrow 3}$
^{30}**SiO**	$v = 1$	$J = 2 \rightarrow 1$
	$v = 2$	$\mathbf{J = 2 \rightarrow 1}$

providing explanations for the maser lines not yet explained; and (*iv*) the overlaps suggesting a search for new maser lines.

• In the first category it is worth mentioning that the overlap of ^{28}SiO $v = 2-1, J = 20-21$ with ^{29}SiO $v = 3-2, J = 8-9$, although it involves relatively high v states for ^{29}SiO, results in strong enhancement of the ^{29}SiO $v = 3, J = 8-7$ transition. This was also predicted by González-Alfonso et al. (1996). We have also verified that two line overlaps, ^{28}SiO $v = 2-1, J = 2-3$ with ^{29}SiO $v = 3-2, J = 11-10$, and ^{29}SiO $v = 3-2, J = 11-10$ with ^{30}SiO $v = 1-0, J = 0-1$, result in a clear enhancement of the ^{29}SiO $v = 3, J = 11 \rightarrow 10$ line intensity. Another example is the enhancement of the ^{30}SiO $v = 2, J = 8 \rightarrow 7$ transition resulting, as in González-Alfonso et al. (1996), from the effects of 3 simultaneous line overlaps.

• We have successfully explained (case (*ii*)) the enhancement of the ^{28}SiO $v = 3, J = 1 \rightarrow 0$ and $v = 4, J = 5 \rightarrow 4$ transitions, and of the ^{30}SiO $v = 0, J = 5 \rightarrow 4$ transition. Standard modelisation does not easily invert the ^{28}SiO $v = 3, J = 1 \rightarrow 0$ line although it is observed in a variety of sources (Scalise & Lépine 1978, Alcolea et al. 1989). One overlap may lead to the excitation of this line: ^{28}SiO $v = 3-2, J = 2-3$ with ^{29}SiO $v = 2-1, J = 5-6$. On the other hand, observations indicate that the ^{28}SiO $v = 3, J = 2-1$ line should be quenched. This could result from four different overlaps including the low J rotation level overlap of ^{28}SiO $v = 2-1, J = 3-4$ with ^{30}SiO $v = 1-0, J = 1-2$. This overlap is also consistent with the extinction of the $v = 3, J = 2-1$ line and with the enhancement of the $v = 4, J = 5 \rightarrow 4$ line as observed by Cernicharo et al. (1993) in VY CMa. Our model easily leads to maser emission of the $v = 0, J = 1 \rightarrow 0$ transition. This is observed in several stars for ^{29}SiO (Alcolea & Bujarrabal 1992) and ^{30}SiO (Cernicharo & Bujarrabal 1992).

• Table 1 (case (*iii*)) and Fig. 3 suggest explanations of the ^{29}SiO and ^{30}SiO maser transitions not explained in the work of González-Alfonso et al. (1996). Only overlaps can explain inversions of the ^{30}SiO $v = 0, J = 2 \rightarrow 1, 4 \rightarrow 3$ (not explained in previous works) or $J = 5 \rightarrow 4$ transitions. Line overlaps are also required to explain several ^{29}SiO $v = 1$ and 2 rotational transitions. For the $v = 1, J = 6 \rightarrow 5$ line observed by Cernicharo & Bujarrabal (1992), Table 1 suggests that it may

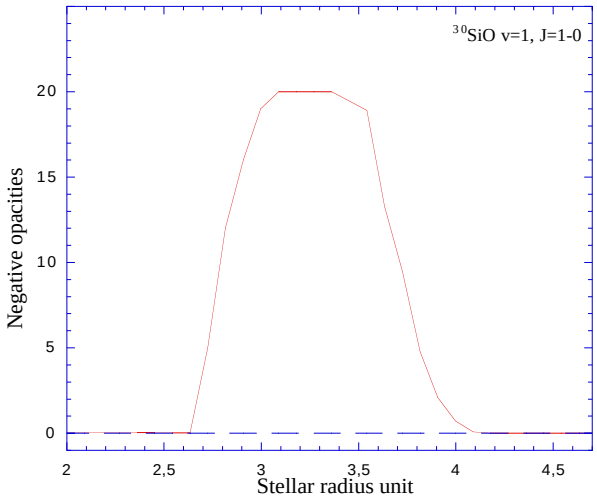

Fig. 4. Negative opacities for the ^{30}SiO $v = 1, J = 1 \rightarrow 0$ maser line with (continuous line) and without (dashed line) overlap, versus the distance to the star (one stellar radius $= 7.7\ 10^{13}$ cm). The overlap used in this computation is given in bold face in Table 1. The H_2 density and the abundance $\chi[SiO/H_2]$ are respectively 10^9 cm^{-3} and $5\ 10^{-5}$ at a distance of $2.8R_\star$.

be explained by several overlaps. Of special interest is the simultaneous overlap of ^{28}SiO $v = 2-1, J = 4-3$ with ^{29}SiO $v = 1-0, J = 1-0$ and of ^{28}SiO $v = 2-1, J = 5-4$ with ^{29}SiO $v = 1-0, J = 2-1$. The same arguments apply to $v = 2, J = 6 \rightarrow 5$ which has also been observed by Cernicharo & Bujarrabal. The overlap of ^{29}SiO $v = 1-0, J = 3-4$ with ^{30}SiO $v = 1-0, J = 1-0$ is clearly important because it enhances simultaneously the observed $J = 4-3$ and $2-1$ transitions. It is interesting to note that we have succeeded in producing weak maser emission in ^{29}SiO $v = 0, J = 5 \rightarrow 4$ (never explained before). Another important result concerns the ^{30}SiO $v = 1, J = 1 \rightarrow 0$ maser emission produced by our model with different overlaps (see Table 1 and Fig. 4); this line was recently discovered by Cho & Ukita (1998) in TX Cam.

• Table 2 lists some relatively strong maser transitions as predicted by our model (case (*iv*)). Note that the ^{29}SiO and ^{30}SiO $v = 1, J = 2 \rightarrow 1$ maser lines have also been predicted by Rausch et al. (1996) on the basis of an optical pumping model. Four transitions (^{28}SiO $v = 4, J = 3 \rightarrow 2$, ^{29}SiO $v = 1, J = 2 \rightarrow 1$ and $v = 3, J = 4 \rightarrow 3$, ^{30}SiO $v = 2, J = 2 \rightarrow 1$) are easily excited even without line overlaps; however, all other transitions require line overlaps for being detectable. For ^{29}SiO $v = 1$ we find that 6 different overlaps of ro-vibrational lines of ^{28}SiO with ^{29}SiO tend to enhance the $J = 5 \rightarrow 4$ transition. Six transitions (given in bold face in Table 2: ^{28}SiO $v = 4, J = 3 \rightarrow 2$, ^{29}SiO $v = 2, J = 1 \rightarrow 0, 3 \rightarrow 2$ and $v = 3, J = 2 \rightarrow 1, 4 \rightarrow 3$, and ^{30}SiO $v = 2, J = 2 \rightarrow 1$) have not yet been searched for maser emission as far as we are aware. However, all other transitions in Table 2 have already been observed without success by several authors (e.g., Cernicharo & Bujarrabal 1992). Nevertheless, further investigations of these lines would be useful, especially

as ^{29}SiO $v = 1, J = 2 \rightarrow 1$ was recently detected in one star (J.R. Pardo, private communication).

Finally, we stress that other types of line overlaps may simultaneously play a role in the anomalous excitation of ^{28}SiO, ^{29}SiO and ^{30}SiO. The infrared lines of water are especially important in this context because water is an abundant species in the late-type stars where SiO is present. Apart from the H_2O-SiO line overlap discussed by Olofsson et al. (1981, 1985) and Bujarrabal et al. (1996), there are several other infrared transitions of ortho- or para-H_2O close to ro-vibrational transitions of SiO and isotopes which would deserve modelisation.

4. Conclusion

We have presented results for a new and simple model of SiO masers which incorporates both radiative and collisional pumpings as well as line overlap effects. Radiative pumping includes stellar radiation and circumstellar grains although their extinction coefficient is not well known. Collisional pumping involves molecular hydrogen as well as atomic hydrogen (under the form of simply guessed H-SiO collision rates). Our model involves 40 rotational levels for each of the first five vibrational states and derives the populations and opacities for the three species ^{28}SiO, ^{29}SiO and ^{30}SiO, and for a variety of circumstellar conditions. Several low and high J rotational transitions are easily inverted in the vibrational states $v = 1, 2, 3$ and 4 as observed in many late-type stars. Prediction of relative line intensities must account for line overlap effects which have been shown to play an important role in the excitation of SiO masers.

Our model incorporates in a very simple way the effects of line overlaps between ro-vibrational lines of ^{28}SiO, ^{29}SiO and ^{30}SiO. Three different overlaps may be treated simultaneously, and we have examined the impact on the level populations and opacities of 31 overlapping line pairs. We have found that line overlaps are important to enhance ^{28}SiO $v = 3, J = 1 \rightarrow 0$ and $v = 4, J = 5 \rightarrow 4$ maser emission or to turn off $v = 3, J = 2 \rightarrow 1$ line emission. Various overlaps may lead to weak ^{29}SiO $v = 0, J = 5 \rightarrow 4$ line emission and strong ^{29}SiO $v = 1$ and 2, $J = 6 \rightarrow 5$ emission; these lines had not been explained in other works. More generally, several ^{29}SiO $v = 1$ and 2 maser lines are well explained with line overlaps. We have also suggested possible explanations to several ^{30}SiO maser lines including the newly discovered transition $v = 1, J = 1 \rightarrow 0$. In addition, we have predicted that several new maser transitions for ^{28}SiO ($v = 4$), ^{29}SiO ($v = 0$ to 3) and ^{30}SiO ($v = 1$ and 2) could result from line overlap effects.

Acknowledgements. We thank the referee, Dr. W.H. Kegel, for useful comments on the manuscript.

References

Alcolea J., Bujarrabal V., Gallego J.D., 1989, A&A 211, 187
Alcolea J., Bujarrabal V., 1992, A&A 253, 475
Bieniek R.J., Green S., 1983, ApJ 265, L29
Bowers P.F., Knapp G.R., 1987, ApJ 315, 305
Bujarrabal V., Nguyen-Q-Rieu Mr., 1981, A&A 102, 65
Bujarrabal V., Planesas P., Gomez-Gonzalez J., Martin-Pintado J., Del Romer, A., 1986, A&A 162, 157
Bujarrabal V., Gomez-Gonzalez J., Planesas P., 1989, A&A 219, 256
Bujarrabal V., 1994, A&A 285, 953
Bujarrabal V., Alcolea J., Sanchez-Contreras C., Colomer F., 1996, A&A 314, 883
Campbell J.M., Klapstein D., Dulick M., Bernath P.F., 1995, A&AS 101, 237
Cernicharo J., Bujarrabal V., Lucas R., 1991, A&A 249, L27
Cernicharo J., Bujarrabal V., 1992, ApJ 401, L109
Cernicharo J., Bujarrabal V., Santaren J.L., 1993, ApJ 407, L33
Cho S.H., Ukita N., 1998, AJ 116, 2495
Doel R.C., Gray M.D., Humphreys E.M.L., Braithwaite M.F., Field D., 1995, A&A 302, 797
Drira I., Huré J.M., Spielfiedel A., Feautrier N., Roueff E., 1997, A&A 319, 720
Elitzur M., 1992, in: Kluwer Academic Publishers (ed.), Astronomical Masers
González-Alfonso E., Alcolea J., Cernicharo J., 1996, A&A 313, L13
González-Alfonso E., Cernicharo J., 1997, A&A 322, 938
Herpin F., 1998, PhD Thesis, Université de Bordeaux 1
Ivezic Z., Elitzur M., 1995, ApJ 445, 415
Langer S.H., Watson W.D., 1984, ApJ 284, 751.
Lockett P., Elitzur M., 1992, ApJ 399, 704
Lucas R., Bujarrabal V., Guilloteau S., et al., 1992, A&A 262, 491
Mathis J.S., 1990, Ann. Rev. Astr. Ap. 28, 37
Netzer N., Elitzur M., 1993, ApJ 410, 701
Olofsson H., Rydbeck O.E.H., Lane A.P., Predmore C.R., 1981, ApJ 247, L81
Olofsson H., Rydbeck O.E.H., Nyman L.-A., 1985, A&A 150, 169
Pardo J.R., 1999, private communication
Rausch E., Kegel W.H., Tsuji T., Piehler G., 1996, A&A 315, 533
Scalise E.Jr., Lépine R.D., 1978, A&A 65, L7
Snyder L.E., Buhl D., 1974, ApJ 189, L31
Sobolev V.V., 1958, in: Ambartsumyan V.A. (ed.), Theoretical Astrophysics, London: Pergamon Press, p. 497
Willson L.A., 1987, in: Kwok S., Pottasch S.R. (eds.), Late Stages of Stellar Evolution, Dordrecht: Reidel, p. 253